Article:
Fernández, A., Jungclaus, A., Doornenbal, P. et al. (26 more authors) (2021) Mirror energy differences above the 0f7/2 shell: First γ-ray spectroscopy of the Tz = −2 nucleus 56Zn. Physics Letters B. 136784. ISSN 0370-2693

https://doi.org/10.1016/j.physletb.2021.136784

Physics Letters B 823 (2021) 136784

Contents lists available at ScienceDirect

Physics Letters B

www.elsevier.com/locate/physletb

Mirror energy differences above the $0f_{7/2}$ shell: First γ-ray spectroscopy of the $T_z = -2$ nucleus ^{56}Zn

A. Fernández [a], A. Jungclaus [a,*], P. Doornenbal [b], M.A. Bentley [c], S.M. Lenzi [d,e], D. Rudolph [f], F. Browne [b], M.L. Cortés [e], T. Koiwai [g,b], R. Taniuchi [c], V. Vaquero [a], K. Wimmer [g,b], T. Arici [h], N. Imai [i], N. Kitamura [i], B. Longfellow [j,k], R. Lozeva [l], B. Mauss [b], D.R. Napoli [e], M. Niikura [g], X. Pereira-Lopez [c], S. Pigliapoco [d], A. Poves [m], F. Recchia [d,e], P. Ruotsalainen [n], H. Sakurai [g], S. Uthayakumaar [c], R. Wadsworth [c], R. Yajzey [c,o]

[a] *Instituto de Estructura de la Materia, CSIC, E-28006 Madrid, Spain*
[b] *RIKEN Nishina Center, 2-1 Hirosawa, Wako, Saitama 351-0198, Japan*
[c] *Department of Physics, University of York, Heslington, York YO10 5DD, United Kingdom*
[d] *Dipartimento di Fisica e Astronomia "Galileo Galilei", Università degli Studi di Padova and INFN Padova, I-35131 Padova, Italy*
[e] *Istituto Nazionale di Fisica Nucleare, Laboratori Nazionali di Legnaro, I-35020 Legnaro, Italy*
[f] *Department of Physics, Lund University, SE-22100 Lund, Sweden*
[g] *Department of Physics, University of Tokyo, 7-3-1 Hongo, Bunkyo, Tokyo 113-0033, Japan*
[h] *GSI Helmholtzzentrum für Schwerionenforschung GmbH, D-64291 Darmstadt, Germany*
[i] *Center for Nuclear Study, University of Tokyo, RIKEN campus, Wako, Saitama 351-0198, Japan*
[j] *Department of Physics and Astronomy, Michigan State University, East Lansing, MI 48824, USA*
[k] *National Superconducting Cyclotron Laboratory, Michigan State University, East Lansing, MI 48824, USA*
[l] *Université Paris-Saclay, IJCLab, CNRS/IN2P3, F-91405 Orsay, France*
[m] *Departamento de Física Teórica and CIAFF, Universidad Autónoma de Madrid, E-28049, Madrid, Spain*
[n] *Department of Physics, University of Jyväskylä, FI-40014 Jyväskylä, Finland*
[o] *Department of Physics, Faculty of Science, Jazan University, Jazan, Saudi Arabia*

ARTICLE INFO

Article history:
Received 23 August 2021
Received in revised form 19 October 2021
Accepted 15 November 2021
Available online 19 November 2021
Editor: B. Blank

ABSTRACT

Excited states in ^{56}Zn were populated following one-neutron removal from a ^{57}Zn beam impinging on a Be target at intermediate energies in an experiment conducted at the Radioactive Isotope Beam Factory at RIKEN. Three γ rays were observed and tentatively assigned to the $6^+ \rightarrow 4^+ \rightarrow 2^+ \rightarrow 0^+$ yrast sequence. This turns ^{56}Zn into the heaviest $T_z = -2$ nucleus in which excited states are known. The excitation-energy differences between these levels and the isobaric analogue states in the $T_z = +2$ mirror partner, ^{56}Fe, are compared with large-scale shell-model calculations considering the full pf valence space and various isospin-breaking contributions. This comparison, together with an analysis of the mirror energy differences in the $A = 58$, $T_z = \pm 1$ pair ^{58}Zn and ^{58}Ni, provides valuable information with respect to the size of the monopole radial and the isovector multipole isospin-breaking terms in the region above doubly-magic ^{56}Ni.

1. Introduction

The exchange symmetry between protons and neutrons is one of the fundamental symmetries of modern physics and led to the concept of isospin in nuclear physics. Isospin symmetry is a consequence of the almost perfect charge independence and charge symmetry of the attractive strong nucleon-nucleon interaction. However, isospin symmetry is naturally broken by the Coulomb force acting between protons. Furthermore, systematic studies of pairs of mirror nuclei, i.e. nuclei with interchanged proton and neutron numbers, over the last two decades have revealed that additional isospin-breaking (ISB) multipole effects exist (see, e.g., Refs. [1–4] and references therein). Most information has been gathered for nuclei in the $0f_{7/2}$ shell, i.e. nuclei in the region between ^{40}Ca and ^{56}Ni [5], as summarized in Fig. 1. While many of these nuclei are rather easily accessible using heavy-ion induced fusion-evaporation reactions in conjunction with highly-efficient γ-ray spectrometers, the most neutron-deficient ones were studied

* Corresponding author.
E-mail address: andrea.jungclaus@csic.es (A. Jungclaus).

https://doi.org/10.1016/j.physletb.2021.136784

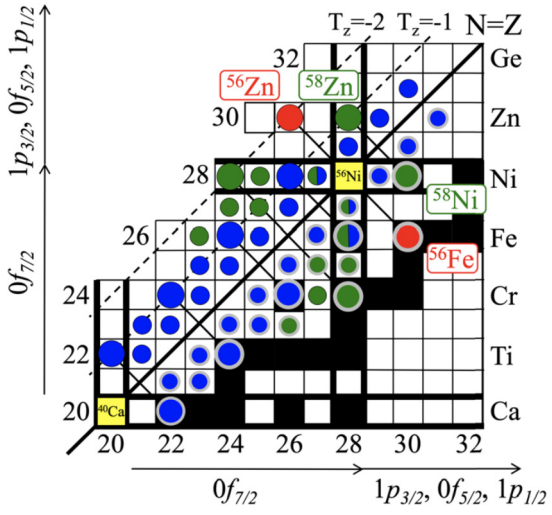

Fig. 1. Overview of isospin-symmetry studies in the region above ^{40}Ca. Mirror pairs studied with fusion-evaporation reactions are shown in blue and those investigated employing in-beam γ-ray spectroscopy at intermediate energies with a ^{58}Ni primary beam at NSCL in green [5]. The $A = 56$, $T_z = \pm 2$ mirror pair subject of the present study is shown in red.

in recent years using in-beam γ-ray spectroscopy at intermediate energies at the National Superconducting Cyclotron Laboratory (NSCL) at Michigan State University [6–12]. On the theoretical side, the nuclei in this region can be described with very good accuracy by the nuclear shell model (SM) when the full pf valence space is considered [2,4]. A systematic comparison between the rich experimental information and shell-model calculations allowed to establish a consistent picture with respect to several isospin-breaking contributions. In particular, it was demonstrated that in order to describe observed differences in excitation energies of states in mirror nuclei, two specific ISB contributions are required besides well-established Coulomb terms, namely the isovector multipole term, V_B, and the monopole radial term, V_{Cr} [1,4,13–15]. In stark contrast, the question how these two additional ISB terms have to be treated above the $0f_{7/2}$ orbital, i.e., in the $Z = N = 28$-50 shell, is still an open question [15,16]. Isospin-symmetry studies of heavier systems therefore often depend on ad hoc assumptions and thus clearly suffer from the lack of decisive data points [15–19].

To tackle this question, we present in this Letter the first γ-ray spectroscopy of ^{56}Zn ($Z = 30$, $N = 26$), which has an isospin projection of $T_z = -2$. An in-beam study of this nucleus is at the very limit of feasibility and became possible only recently due to the availability of a high-intensity ^{78}Kr primary beam at the Radioactive Isotope Beam Factory (RIBF) at RIKEN. The observation of three γ rays, emitted from excited ^{56}Zn ions produced via one-neutron removal from a ^{57}Zn beam at intermediate energies, allowed to establish the yrast sequence of this nucleus. ^{56}Zn, as well as its $T_z = +2$ mirror nucleus ^{56}Fe and the $T_z = \pm 1$ pair ^{58}Zn/^{58}Ni, has only two nucleons outside the $0f_{7/2}$ shell (see Fig. 1). Therefore, the influence of the next orbital, $0g_{9/2}$, which quickly increases when more and more nucleons are added above ^{56}Ni, is still small and these nuclei are still well described by SM calculations in the pf space. The $A = 56$, $T_z = \pm 2$ and $A = 58$, $T_z = \pm 1$ mirror pairs thus offer a unique opportunity to pin down the contributions of the $1p$, $0f_{5/2}$ orbitals to the V_B and V_{Cr} terms in the upper pf shell.

2. Experiment and results

The experiment was conducted at the RIBF, operated by the RIKEN Nishina Center and the Center for Nuclear Study of the University of Tokyo. A ^{78}Kr primary beam with an average intensity of 300 pnA and an energy of 345 MeV/nucleon underwent fragmentation on a 7-mm thick Be target. During their passage through the BigRIPS spectometer [20], the constituents of the resulting cocktail beam were identified based on their charge (Z) and mass-to-charge ratio (A/Q) by means of the $B\rho$-ΔE-TOF method [21]. The magnetic rigidity, $B\rho$, the time-of-flight, TOF, and the energy loss, ΔE, were determined on an event-by-event basis thus enabling a complete identification of the beam components. The ^{57}Zn ions, which followed a central trajectory in BigRIPS, reached the 6-mm thick Be secondary reaction target placed in the final focal plane of BigRIPS with an energy of 200 MeV/nucleon, translating into a mid-target velocity of $\beta = 0.51$. The secondary reaction products were identified via the measurement of $B\rho$, TOF, and ΔE in the ZeroDegree spectrometer [20], leading to an unambiguous selection of reaction residues. To detect γ radiation emitted following the nuclear reactions, the reaction target was surrounded by the DALI2+ spectrometer [22] which was composed of 226 NaI crystals covering polar angles in the range $\theta = 18°$-$125°$ with respect to the beam axis. The individual crystals were calibrated in the energy range of interest using ^{88}Y, ^{60}Co, and ^{137}Cs sources. The response of the array to in-flight decays was simulated using the Geant4 toolkit [23]. A photo-peak efficiency of 15% and a resolution after Doppler correction of 11% (FWHM) were obtained for 1.3 MeV γ rays emitted at $\beta = 0.51$. Confidence intervals for the γ-ray energies and absolute intensities were extracted by means of a χ^2 minimization following the maximum-likelihood method for Poisson-distributed, binned data [24], and using model responses from the Geant4 simulation. Systematic uncertainties in the deduced model parameters and the geometry of the experimental setup were characterized using well-known transitions in ^{52}Fe and ^{54}Ni, nuclei which were populated in the same experiment. The target position relative to the DALI2+ array deduced from the fit of known γ rays emitted from excited states with negligible half-lives was found to be in good agreement with the measured physical location. The accuracy obtained for the extracted γ-ray energies was better than 0.4%. This additional uncertainty was propagated accordingly in the γ-ray energy uncertainties reported below. For more details regarding the data analysis we refer to Ref. [25].

The prompt Doppler-corrected γ-ray spectrum of ^{56}Zn, populated via one-neutron removal from ^{57}Zn, is presented in Fig. 2(a). The spectrum was adjusted in the range between 400 and 2500 keV including three DALI2+ response functions simulated for γ-ray energies of 830, 1272, and 1380 keV. A smooth background was represented by a double-exponential function. Although the full-energy peaks of the 1272-keV and 1380-keV γ rays were not resolved, the occurrence of a well-defined global minimum for the two transitions was verified by a χ^2 test in terms of the γ-ray energies and intensities of the doublet. Correlations between the model parameters were accounted for by minimizing the χ^2 as a function of the remaining parameters describing the doublet [25]. The resulting χ^2 matrix for the energies is presented in the inset of Fig. 2(a). The confidence intervals are taken as the extremes of the 1σ contour in the multi-parameter χ^2 surfaces. The resulting γ-ray energies for the three observed transitions are 830(5), 1272(13), and 1380(16) keV. The lifetimes of all relevant excited states in ^{56}Zn are expected to be $\tau \leq 10$ ps based on a comparison with the $T_z = +2$ mirror nucleus ^{56}Fe [26]. This lifetime limit translates into an uncertainty of <1 keV for the transition energy when $\tau = 0$ ps is assumed in the simulations. For the relative intensities, values of 100(5), 76(19), and 58(11)%, respectively, were obtained from the χ^2 analysis. Independent evidence for the doublet structure of the broad peak around 1.3 MeV in Fig. 2(a) is provided by inspection of the background-corrected γ-γ coincidence spectra shown in Fig. 2(b). When selecting the left part of the doublet, the higher-energy component is observed in coincidence and vice versa. Furthermore, in both coincidence spectra a

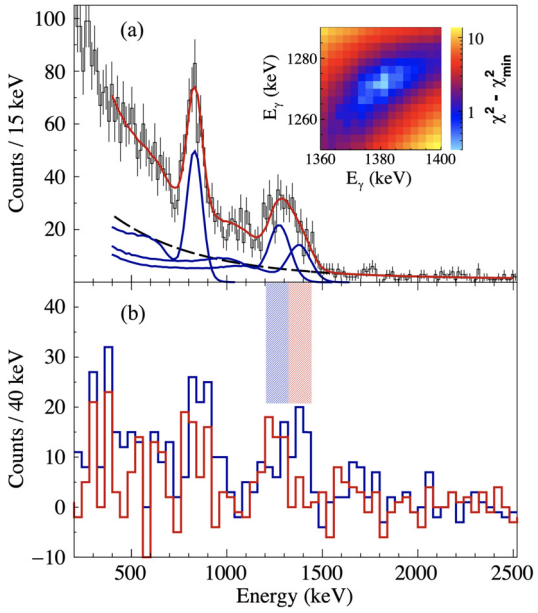

Fig. 2. (a) Prompt γ-ray energy spectrum of ^{56}Zn populated via one-neutron removal from ^{57}Zn. Only events in which less than five DALI2+ crystals fired were included. The red line represents the best fit of the spectrum. The simulated lineshapes composing the fit are depicted in blue. The black dashed line represents the double-exponential background. The χ^2 matrix for the γ-ray energies of the 1272-1380-keV doublet is shown in the inset. (b) Background-subtracted γ-γ coincidence spectra for the left (blue) and right (red) part of the doublet, respectively.

line at 830 keV is visible. Thus, the three transitions are observed in mutual coincidence and it can be concluded that they form a γ-ray cascade. The ordering of the transitions within the cascade was established on the basis of the experimental intensities. For the resulting excited states at energies of 830(5), 2102(14), and 3482(21) keV tentative spin and parity assignments of (2^+), (4^+), and (6^+), respectively, are proposed based on the analogy to the mirror nucleus ^{56}Fe, which is illustrated in Fig. 3.

3. Discussion

To analyze the experimental findings, large-scale shell-model calculations were performed for the $A = 56$, $T_z = \pm 2$ mirror pair and the $T_z = \pm 1$ nuclei ^{58}Zn and ^{58}Ni. The latter form the only other even mirror pair with only either protons or neutrons above the $N = Z = 28$ gap for which experimental mirror energy differences (MED) are available. In addition, the population of excited states in ^{56}Zn via one-neutron removal from ^{57}Zn was calculated. The shell-model code ANTOINE [27,28] was used and the full pf valence space was employed, comprising the $0f_{7/2}$, $1p_{3/2}$, $1p_{1/2}$, and $0f_{5/2}$ orbitals above the ^{40}Ca core. Due to computational limitations, the calculations for the $A = 57$, 58 nuclei had to be constrained to $t = 8$ particle-hole excitations across the $N = Z = 28$ shell gaps. No restrictions were applied at $A = 56$. The calculations were performed with the KB3GR [29] effective interaction. As compared to its precursor, the well-established KB3G interaction [30,2], KB3GR features an improved description of the interaction among the $1p_{3/2}$, $1p_{1/2}$, and $0f_{5/2}$ orbitals which was derived from a fit to the energies of about 200 excited states of nuclei with N or Z in the range 28 to 32. Due to the way it was constructed, this interaction is considered best suited for the study of the $A = 56$, 58 nuclei under discussion in the present work. For the calculation of transition probabilities bare g factors and effective nucleon charges $\varepsilon_p = 1.15e$ and $\varepsilon_n = 0.80e$ were used for protons and neutrons, respectively [31]. Fig. 3 shows the level scheme calculated with the isospin-conserving KB3GR interaction for the $A = 56$, $T_z = \pm 2$ nuclei in comparison with experimental information. We note that

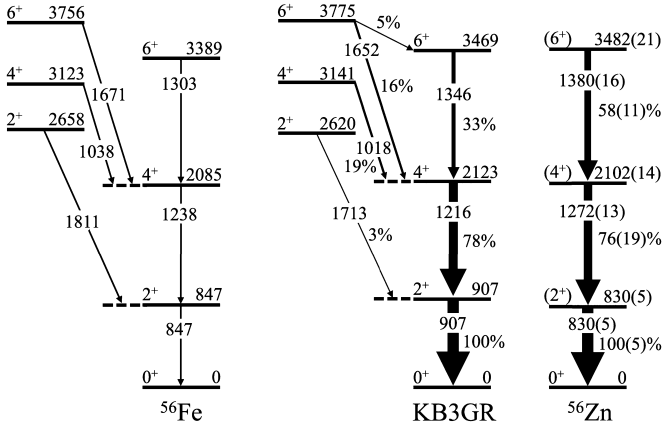

Fig. 3. Partial level scheme of ^{56}Fe [26] (left), KB3GR shell-model prediction for $A = 56$, $T_z = \pm 2$ (middle), and yrast sequence of ^{56}Zn as observed in the present work (right).

the known decay pattern of the non-yrast states in ^{56}Fe nicely agrees with the shell-model expectation based on the calculated electromagnetic decay properties. The observed relative intensities of the three γ rays connecting the yrast line in ^{56}Zn are also consistent with those estimated from the calculated branching ratios and spectroscopic factors for one-neutron removal from ^{57}Zn assuming constant single-particle reaction cross sections.

To study mirror energy differences, isospin-breaking terms have to be included in the shell-model calculations. Here, we follow the terminology and prescription of Ref. [4]. First, we add the Coulomb multipole matrix elements, V_{CM}, to the nuclear ones and adjust the single-particle proton and neutron energies taking into account the electromagnetic spin-orbit, $V_{\ell s}$, and orbit-orbit, $V_{\ell\ell}$, corrections. After diagonalizing this interaction in the model space for both mirror partners, we compute the expectation value of the schematic isospin-breaking isovector term, V_B. This term was originally introduced for the $0f_{7/2}$ shell, where $V_B^2 = +100$ keV was applied to the $J = 2$ coupling [1,3,4]. Later, it was shown that equivalent results are obtained applying either V_B^2 to the $J = 2$ or $V_B^0 = -V_B^2$ to the $J = 0$ matrix element [14]. The latter approach has the important advantage of allowing to consider this term on an equal footing for all orbitals of the valence space [15,32,19]. For the mass range $A = 51$-54, i.e. the heaviest $0f_{7/2}$-shell nuclei, a best value of $V_B^0 = -71(3)$ keV was deduced from the experimental data [14]. Here, this strength is applied to either only the $0f_{7/2}$ orbital or all four orbitals of the valence space in order to investigate the contribution of the $1p$ and $0f_{5/2}$ orbitals to this term. Finally, we add to the MED the radial term, V_{Cr}, that takes into account state-dependent changes in the nuclear radius. Since low-ℓ orbits in a shell have larger radii than higher-ℓ ones, changes in the relative occupation of these orbits modify the radius [1,4]. In the study of nuclei in the $0f_{7/2}$ shell, usually only the occupancy of the $1p_{3/2}$ orbital, which typically is far below one nucleon, is considered with a standard strength parameter $\alpha = 200$ keV [4]. Recently, however, it has been shown that when a low-ℓ orbit is occupied by more than one nucleon its radius decreases considerably [33,34]. In the case of the sd shell, the difference between the root-mean-square radii of the $1s_{1/2}$ and $0d$ orbitals, ρ_s-ρ_d, reduces around $A \approx 28$ by a factor of 2.5-3.0 [34]. In the nuclei under study here, the occupancy of the $1p_{3/2}$ orbital is typically in the range 1.5-2.0. It is thus expected that a smaller value of α, as compared to the standard value, would be more appropriate in the present cases. Since the decrease of ρ_p-ρ_f upon filling of the $1p_{3/2}$ orbital is not known, calculations were made for values of $\alpha = 0$, 50, 100, and 200 keV in order to derive the best value of α for nuclei in the upper pf shell from a comparison to the experimental data.

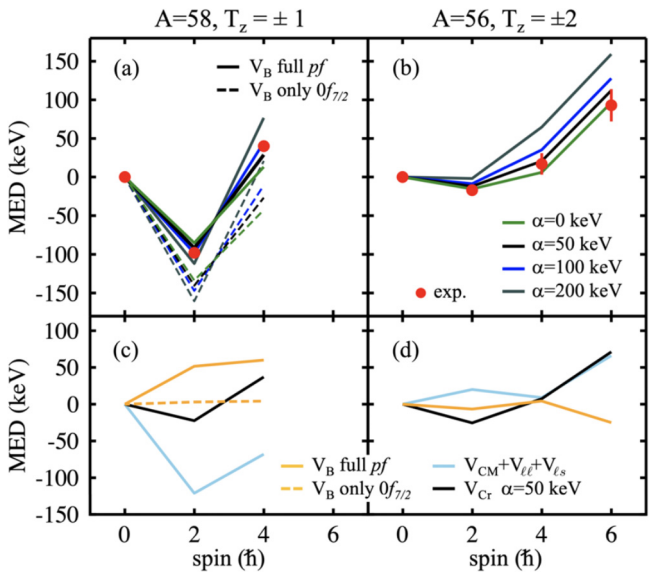

Fig. 4. Comparison of experimental MED (red dots, from Ref. [5] and the present work) with the results of shell-model calculations with the KB3GR interaction for (a) the $A = 58$, $T_z = \pm 1$ and (b) the $A = 56$, $T_z = \pm 2$ mirror pair. Predictions are shown for $\alpha = 0$ keV (green), 50 keV (black), 100 keV (blue), and 200 keV (gray) for the $1p_{3/2}$ orbital and, for the $A = 58$ pair, $V_B^0 = -71$ keV applied to either all pf orbitals (solid lines) or only to the $0f_{7/2}$ (dashed lines). Panels (c) and (d) show the individual contributions to the MED. See text for details. Experimental data are taken from Ref. [5] and the present work.

For the $1p_{1/2}$ orbital with occupancies <0.5, the standard value $\alpha = 200$ keV is used [15,33,35].

The predicted MED for the two mirror pairs of interest are compared with the experimental results in Figs. 4(a) and (b), while Figs. 4(c) and (d) show the individual contributions to the calculated MED. These are the Coulomb contribution, V_{CM}, coupled to the multipole Coulomb single-particle shifts, $V_{\ell\ell}$ and $V_{\ell s}$, the additional isovector term, V_B, and the radial term, V_{Cr}. Fig. 4(a) evidences that the $A = 58$ pair is particularly sensitive to the contribution of the orbitals of the upper pf shell to the isovector term, V_B. In these nuclei, the $0f_{7/2}$ shell is nearly completely filled, so that the contribution of this orbital to V_B vanishes, see Fig. 4(c). In contrast, large values of around $V_B \approx 50$ keV are expected for the 2^+ and 4^+ states when this correction is applied for all orbitals of the valence space. The dependence of the MED on the value of α, on the other hand, is very small for this mirror pair as shown in Fig. 4(a). The comparison between experimental and calculated MED shown in that figure therefore clearly demonstrates that the contribution of all pf orbitals to the V_B term has to be taken into account in order to reproduce the experimental data.

Having settled the correct treatment of the V_B term, we can now proceed to investigate the size of the radial term, V_{Cr}. This monopole term scales with the difference in Z of the mirror partners. The new experimental data on the $A = 56$, $T_z = \pm 2$ pair therefore offer a unique opportunity to estimate the strength parameter α for the $1p_{3/2}$ orbital in the region above the $0f_{7/2}$ shell, i.e. for nuclei in which the occupancy of this orbital significantly exceeds one nucleon. As seen in Fig. 4(d), the SM calculations yield only small Coulomb and V_B contributions up to the 4^+ state. This is expected considering the particle-hole symmetry of these nuclei having one pair of nucleons and one pair of holes with respect to ^{56}Ni. Furthermore, $V_{CM} + V_{\ell\ell} + V_{\ell s}$ and V_B have opposite sign and nearly cancel for all states. It is thus mainly the radial term, V_{Cr}, which determines the trend of the MED curve, as observed by comparing Figs. 4(b) and (d). Best agreement between experimental and calculated MED is found for a value of α around 50 keV or even below, a value which is significantly smaller as compared to that commonly used for nuclei in the $0f_{7/2}$ shell. This finding constitutes first evidence that the radius of the $1p_{3/2}$ orbital decreases considerably when it is occupied by more than one nucleon. A similar behavior of the $1s_{1/2}$ orbital was recently discussed in Ref. [34]. To conclude the discussion of Fig. 4, based on the comparison between the measured and theoretical MED the magnitude of the V_B and V_{Cr} terms in the region above the $0f_{7/2}$ shell could be determined and thereby the open question raised in the introduction answered.

4. Summary

To summarize, we reported on the first γ-ray spectroscopic study of ^{56}Zn which allowed to establish the yrast sequence of this $T_z = -2$ nucleus up to the 6^+ state. The mirror energy differences for the $A = 56$, $T_z = \pm 2$, and $A = 58$, $T_z = \pm 1$, pairs were compared with shell-model calculations performed using the full pf valence space and the KB3GR effective interaction. This comparison has put in evidence that the experimental data can only be reproduced when the isovector multipole term, V_B, is considered on equal footing for all orbitals of the valence space, not only the $0f_{7/2}$ shell. Furthermore, it has shown that the contribution of the $1p_{3/2}$ orbital to the radial term, V_{Cr}, is significantly quenched due to the decrease of its radius once its occupancy exceeds one nucleon. We note that these results, which set the basis for future studies of isospin symmetry in the upper pf shell, were obtained under the presumption that for the nuclei discussed in the present work the influence of the $0g_{9/2}$ orbital is negligible.

Declaration of competing interest

The authors declare that they have no known competing financial interests or personal relationships that could have appeared to influence the work reported in this paper.

Acknowledgements

We thank the RIKEN Nishina Center accelerator staff and the BigRIPS team for providing excellent beams to the experiment. This work was supported by the Spanish Ministerio de Ciencia e Innovación under contracts FPA2017-84756-C4-2-P, PGC-2018-94583, and SEV-2016-0597, the Swedish Research Council (Vetenskapsrådet, VR 2016-3969), and the UK Science and Technology Facilities Council (STFC) under grants ST/L005727/1 and ST/P003885/1. FB is supported by the RIKEN Special Postdoctoral Researcher Program.

References

[1] A.P. Zuker, S.M. Lenzi, G. Martínez-Pinedo, A. Poves, Phys. Rev. Lett. 89 (2002) 142502.
[2] E. Caurier, G. Martínez-Pinedo, F. Nowacki, A. Poves, A.P. Zuker, Rev. Mod. Phys. 77 (2005) 427.
[3] J. Ekman, C. Fahlander, D. Rudolph, Mod. Phys. Lett. A 20 (2005) 2977.
[4] M.A. Bentley, S.M. Lenzi, Prog. Part. Nucl. Phys. 59 (2007) 497.
[5] https://www.nndc.bnl.gov/ensdf.
[6] J.R. Brown, et al., Phys. Rev. C 80 (2009) 011306(R).
[7] P.J. Davies, M.A. Bentley, T.W. Henry, E.C. Simpson, A. Gade, S.M. Lenzi, et al., Phys. Rev. Lett. 111 (2013) 072501.
[8] C. Langer, F. Montes, A. Aprahamian, D.W. Bardayan, D. Bazin, B.A. Brown, et al., Phys. Rev. Lett. 113 (2014) 032502.
[9] S.A. Milne, M.A. Bentley, E.C. Simpson, T. Baugher, D. Bazin, J.S. Berryman, et al., Phys. Rev. Lett. 117 (2016) 082502.
[10] S.A. Milne, M.A. Bentley, E.C. Simpson, P. Dodsworth, T. Baugher, D. Bazin, et al., Phys. Rev. C 93 (2016) 024318.
[11] M. Spieker, A. Gade, D. Weisshaar, B.A. Brown, J.A. Tostevin, B. Longfellow, et al., Phys. Rev. C 99 (2019) 051304(R).
[12] M. Spieker, D. Weisshaar, A. Gade, B.A. Brown, P. Adrich, D. Bazin, et al., Phys. Rev. C 100 (2019) 061303(R).

[13] S.M. Lenzi, N. Marginean, D.R. Napoli, C.A. Ur, A.P. Zuker, G. de Angelis, A. Algora, M. Axiotis, et al., Phys. Rev. Lett. 87 (2001) 122501.
[14] M.A. Bentley, S.M. Lenzi, S.A. Simpson, C.Aa. Diget, Phys. Rev. C 92 (2015) 024310.
[15] S.M. Lenzi, R. Lau, J. Phys. Conf. Ser. 580 (2015) 012028.
[16] K. Kaneko, Y. Sun, T. Mizusaki, S. Tazaki, Phys. Rev. Lett. 110 (2013) 172505.
[17] K. Kaneko, S. Tazaki, T. Mizusaki, Y. Sun, M. Hasegawa, G. de Angelis, Phys. Rev. C 82 (2010) 061301(R).
[18] P. Ruotsalainen, D.G. Jenkins, M.A. Bentley, R. Wadsworth, C. Scholey, K. Auranen, et al., Phys. Rev. C 88 (2013) 041308(R).
[19] S.M. Lenzi, A. Poves, A.O. Macchiavelli, Phys. Rev. C 102 (2020) 031302(R).
[20] T. Kubo, et al., Prog. Theor. Exp. Phys. 2012 (2012) 03C003.
[21] N. Fukuda, T. Kubo, T. Ohnishi, N. Inabe, H. Takeda, D. Kameda, H. Suzuki, Nucl. Instrum. Methods B 317 (2013) 323.
[22] S. Takeuchi, T. Motobayashi, Y. Togano, M. Matsushita, N. Aoi, K. Demichi, H. Hasegawa, H. Murakami, Nucl. Instrum. Methods A 763 (2014) 596.
[23] S. Agostinelli, et al., Nucl. Instrum. Methods A 506 (2003) 250.
[24] S. Baker, R.D. Cousins, Nucl. Instrum. Methods 221 (1984) 437.
[25] A. Fernández Martínez, PhD thesis, Universidad Autónoma de Madrid, 2021.
[26] H. Junde, H. Su, Y. Dong, Nucl. Data Sheets 112 (2011) 1513.
[27] E. Caurier, Shell-model code ANTOINE, IRES, Strasbourg, 1989-2002.
[28] E. Caurier, F. Nowacki, Acta Phys. Pol. 30 (1999) 705.
[29] E. Caurier, A. Poves, Unpublished.
[30] A. Poves, J. Sánchez-Solano, E. Caurier, F. Nowacki, Nucl. Phys. A 694 (2001) 157.
[31] R. du Rietz, J. Ekman, D. Rudolph, C. Fahlander, A. Dewald, O. Möller, et al., Phys. Rev. Lett. 93 (2004) 222501.
[32] A. Boso, S.M. Lenzi, F. Recchia, J. Bonnard, A.P. Zuker, S. Aydin, et al., Phys. Rev. Lett. 121 (2018) 032502.
[33] J. Bonnard, S.M. Lenzi, A.P. Zuker, Phys. Rev. Lett. 116 (2016) 212501.
[34] J. Bonnard, A.P. Zuker, J. Phys. Conf. Ser. 1023 (2018) 012016.
[35] S.M. Lenzi, M.A. Bentley, R. Lau, C.Aa. Diget, Phys. Rev. C 98 (2018) 054322.